Venus: Atmospheric Motion and Structure from Mariner 10 Pictures

Abstract. *The Mariner 10 television cameras imaged the planet Venus in the visible and near ultraviolet for a period of 8 days at resolutions ranging from 100 meters to 130 kilometers. The general pattern of the atmospheric circulation in the upper tropospheric/lower stratospheric region is displayed in the pictures. Atmospheric flow is symmetrical between north and south hemispheres. The equatorial motions are zonal (east-west) at approximately 100 meters per second, consistent with the previously inferred 4-day retrograde rotation. Angular velocity increases with latitude. The subsolar region, and the region downwind from it, show evidence of large-scale convection that persists in spite of the main zonal motion. Dynamical interaction between the zonal motion and the relatively stationary region of convection is evidenced by bowlike waves.*

On 5 February 1974, Mariner 10, carrying two television cameras, crossed the Venus terminator from the dark side, swinging around the planet on a hyperbolic trajectory on its way to Mercury (*1*). The cameras were designed mainly to observe the surface details of Mercury (*2*); however, the optical design incorporated special filters, coatings, and transmitting glass in order to image Venus in the ultraviolet (UV).

Faint UV markings (Fig. 1) were discovered on Venus in 1926 by Ross (*3*). Decades of subsequent UV observations from the earth suggest a retrograde equatorial motion with a 4-day period (approximately 100 m/sec) (*4*). At least one feature (which takes the form of a dark horizontal Y) appears to be quasi-permanent (*5*) or recurrent (*6*). Spectroscopically observed Doppler shifts in reflected sunlight (*7*) suggest retrograde equatorial motions of approximately 100 m/sec (at pressure levels near ~ 200 mbar). In situ measurements lower in the atmosphere, from Venera 8, are also consistent with these inferred motions (*8*). From studies of optical phenomena near inferior conjunction, Goody (*9*) places the tops of the clouds at altitudes lower than about the 10-mbar pressure level. Rayleigh scattering alone due to the primary atmospheric constituent, CO_2, would limit visibility of features in the UV to altitudes well above the 400-mbar level (*10*). Hence, the UV markings probably (i) originate in the same general region of the atmosphere as the spectroscopically observed Doppler shifts and (ii) reflect mainly mass motion in the atmosphere rather than propagating waves.

The television images returned from Mariner 10 cover the global development of the UV markings over an 8-day period, approximately two rotation periods of the troposphere/lower stratosphere region. Our sample of the dynamical regime on Venus is thus limited vertically and temporally. Nevertheless, the Mariner 10 pictures contain a surprising amount of information about the general circulation of this part of the atmosphere, which will enhance the value of ground-based observations as well as establish a specific scientific framework for future entry probes and orbiters.

In brief, the pictures display highly symmetrical motions relative to the rotational axis encompassing both north and south hemispheres; angular velocity increases with latitude. Zonal flow near the equator is consistent with an approximately 4-day retrograde rotation period. An unexpected equatorial disturbance continually develops near the subsolar point, within which cellular structures suggestive of convection are exhibited. There is dynamical in-

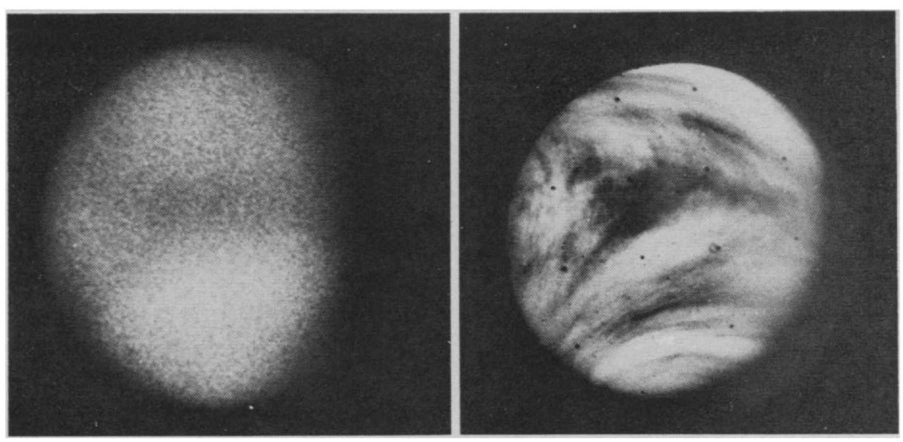

Fig. 1. A Y-shaped feature can be seen in UV light. The picture at the left was taken at the Pic du Midi Observatory, France (04:47 U.T., 24 July 1966); it has a resolution of about 500 km. By contrast, the Mariner 10 picture at the right was taken from 3,300,000 km (03:57 U.T., 10 February 1974); it has a resolution of 65 km.

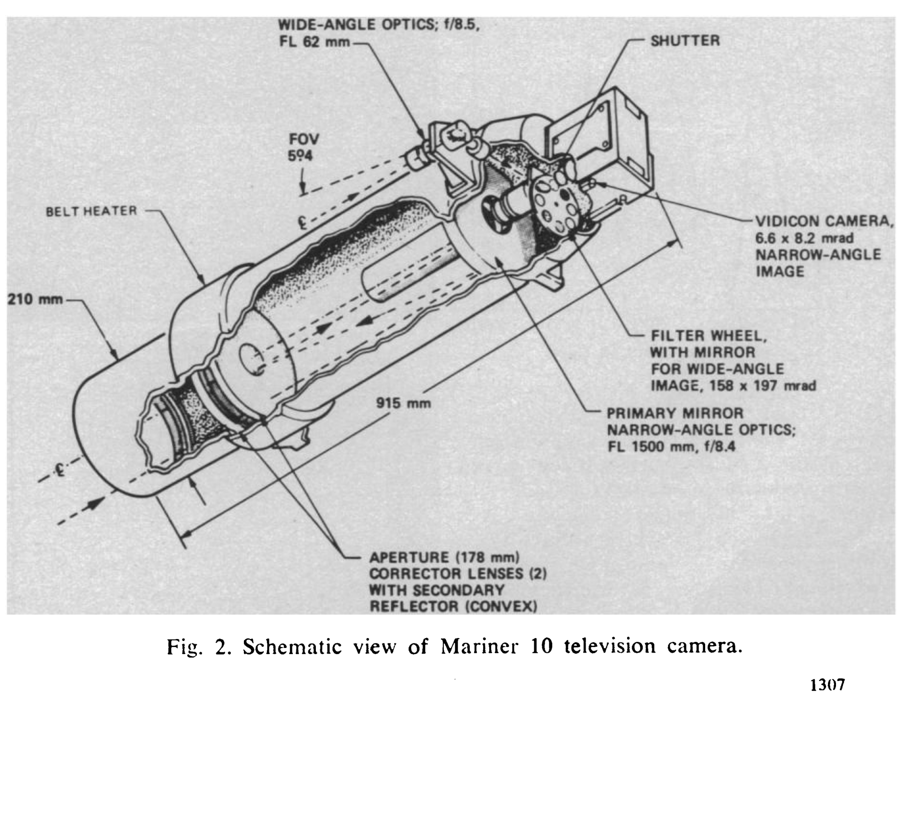

Fig. 2. Schematic view of Mariner 10 television camera.

Table 1. Filter characteristics, calculated for a sample selenium vidicon using the spectral radiance of Venus.

Filter	Effective wavelength (Å)
Ultraviolet	3550
Blue	4740
Orange	5780
Clear	4820
Minus ultraviolet	5120
Ultraviolet polarizing	3580

Table 2. Television performance characteristics.

Characteristic	Value
Focal length	1500 mm
f/number	f/8.4
Field of view	0.36° × 0.48°
Sensor dimension	9.6 × 12.35 mm
Format in pixels	700 × 832
Encoding	8 bits
Frame time	42 seconds
Resolution per television line	9.5×10^{-6} radians

teraction between this solar-oriented equatorial disturbance and the main zonal flow. Bright jetlike streams spiral around the planet to merge into a conspicuous circumpolar band.

Experiment description. The Mariner 10 television hardware and operations are similar to the Mariner 9 (Mars, 1971) system (*11*). Several significant improvements, however, have been made as a result of past experience and the unique requirements of this mission. Besides the extension of spectral response into the UV, the most important change for the study of Venus is a dramatic increase in the communications band width from 16 to 117.6 kbit/sec. As a result, tape storage on the spacecraft could be bypassed. Near the planet every frame acquired was transmitted in real time, making possible high-resolution time lapse studies.

To take full advantage of the Mercury trajectory, new optics with a 1500-mm focal length were developed with extended blue and UV response. The field of view is 0.36° by 0.48°. Table 1 gives the characteristics of the filters which were included with each camera, and a schematic of the system is presented in Fig. 2. Figure 3 illustrates the relative spectral response of the filter/camera combination for the primary filters used in the Venus sequence.

Each television frame consists of 700 scan lines, each of which is sampled 832 times. These samples are encoded to 256 discrete levels (8 bits). Table 2 briefly describes basic characteristics of the overall system. Two cameras are employed, with one camera reading out its image while the other is being prepared. Residual image (a low-level signal remaining from an earlier image) has been virtually eliminated by vidicon faceplate light flooding between each read and erase cycle. Changes to the high-voltage power supply and deflection/focus coil assemblies have reduced electronic noise and readout distortion.

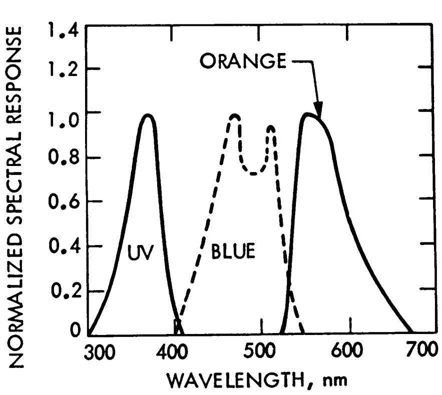

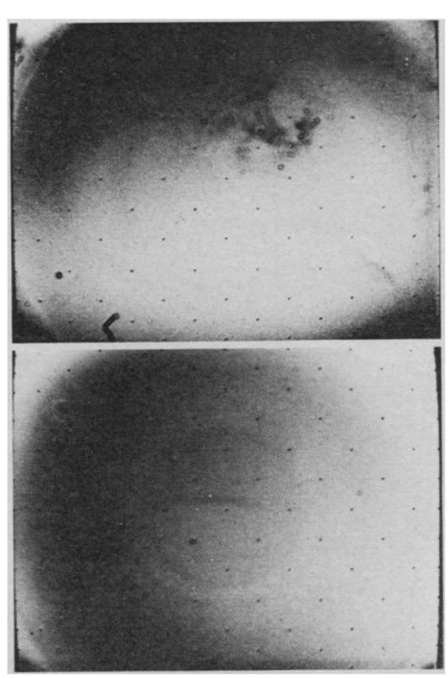

Fig. 3 (left). Relative spectral response curves of the filter/camera combination used in the Venus sequence. Each curve is independently normalized. Fig. 4 (right). Flat-field images from the "A" camera (top) and "B" camera (bottom), contrast-enhanced to map and illustrate artifacts and blemishes that are present in the pictures.

The flat-field signal-to-noise ratio of the cameras is better than 200 to 1. At the limiting spatial resolution, 4.5 arc seconds, the signal-to-noise ratio is better than 20 to 1. As a result, extremely low contrast scenes can be resolved through appropriate computer spatial filtering and contrast enhancing of the digital data. Discernible tonal variations in pictures accompanying this report sometimes reflect intrinsic brightness variations of less than 1 percent. As a consequence of this unparalleled discriminability, faint blemishes introduced into the pictures by the imaging system itself are made visible through computer processing. Figure 4 shows sample images which have been greatly enhanced to illustrate the artifacts. The small black squares are reseau marks to permit computer restoration of geometric integrity to the images.

Figure 5 illustrates the Venus encounter sequence through the first 20 hours past encounter, during which continuous picture-taking was carried out. From 1 to 4 days after encounter, mosaics in the UV were obtained at 2-hour intervals. Between 4 and 6 days the images were taken at 8-hour centers, and on the 7th and 8th days 12-hour intervals were used (*12*). The spatial resolution at cessation of photography was 130 km, which is about twice the best Earth-based resolution.

About 3400 useful frames were acquired, but fewer than half of these have been processed and studied so far. Figure 6 illustrates the "footprints" of the frames on the planet for the highest-resolution mosaic, which has not yet been reconstructed. Most of the preliminary results included in this report have been obtained from mosaics of frames taken 1 day out and later.

In the description of atmospheric motions it is often useful to refer to the points of the compass and also to draw analogy with motions on the earth. On Venus, however, rotation is in a retrograde sense. We refer here to north as in the direction of the north ecliptic pole. Thus we must accept a left-hand rotation convention. All pictures here are printed with north at the top. Rotation is from right to left, and the right-hand edge of the disk is the morning terminator.

Description of the observed markings. Venus has been observed through all of the filters. In the blue and orange, very faint global scale markings may be present occasionally, but these frames have not yet been studied in detail. Hence, we restrict discussion to UV

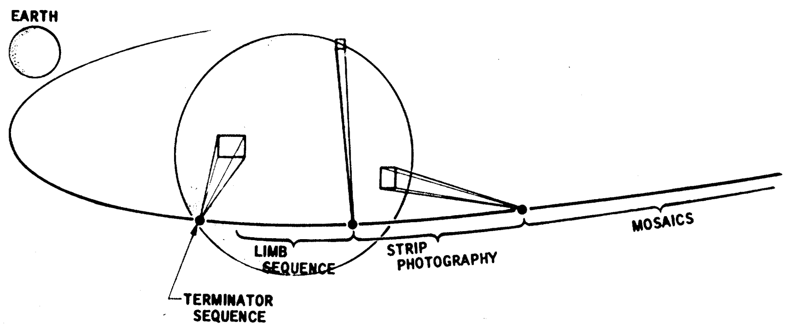

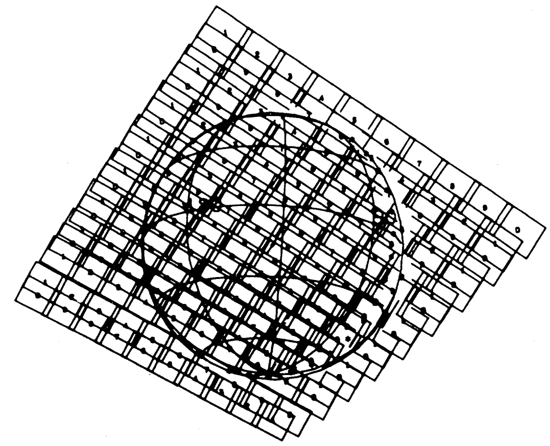

Fig. 5 (left). Picture sequences at near encounter were designed to obtain data concerning specific questions and later to monitor the entire planet. Fig. 6 (right). "Footprints" of a multiframe mosaic in the Venus sequence, taken about 6½ hours after encounter.

pictures and to certain pictures of the planetary limb taken through the orange filter.

The UV images have three general characteristics: (i) a mottled appearance full of small-scale (100 to 500 km) features found in the equatorial zone surrounding the subsolar point (Fig. 7, top; Fig. 8); (ii) streaky and banded structures in the higher latitudes of both hemispheres (Fig. 7, bottom; Figs. 9 and 10); and (iii) a strongly divergent flow pattern around the subsolar point and symmetrical about the equator (Figs. 9, 10, and 11). These patterns are evident in all of the global pictures and mosaics. Figure 12 illustrates the global aspect of the planet from 1 to 8 days after encounter.

The major light and dark markings on the surface of the planet, which have dimensions of the order of 1000 km, are found to be composed of a wealth of smaller-scale features with dimensions down to about 10 km. The maximum contrast detected so far between the major light and dark UV regions is about 30 percent, consistent with Earth-based observations (*13*). Brightness differences of 5 to 10 percent are found in the mottled areas and in the streaks with dimensions of more than several hundred kilometers. The smallest resolvable dark streaks, 10 to 20 km wide, differ by only 2 to 5 percent from the surrounding background.

The lifetimes of the various light and dark markings between ± 50° latitude are variable. Preliminary estimates are illustrated in Figs. 8 and 10. Both large and small features (~ 200 to 1200 km) can retain their basic geometrical configuration during passage across the disk almost from terminator to limb, implying lifetimes in excess of 12 hours. Features a few hundred kilometers in diameter can persist for a period of 2 hours in some cases or, alternatively, can become unrecognizable over the same time period. Many fine-scale (50 to 100 km) cellular features in the vicinity of the subsolar point became unrecognizable in a period at least as short as 2 hours, the time interval between consecutive mosaics; however, overlapping frames within the same mosaic exhibit lifetimes greater than 15 minutes in some cases.

Characteristics of the observed circulation. We are confident from the nature of the spatial patterns and temporal variations of the UV markings that global atmospheric motions are being recorded. Analysis of vertical structure (discussed later) suggests that the markings probably originate within the visible cloud region encompassing the stratosphere and upper troposphere of Venus. The sharp spectral dependence of the markings suggests variation in absorptivity rather than particle size as the primary optical process involved.

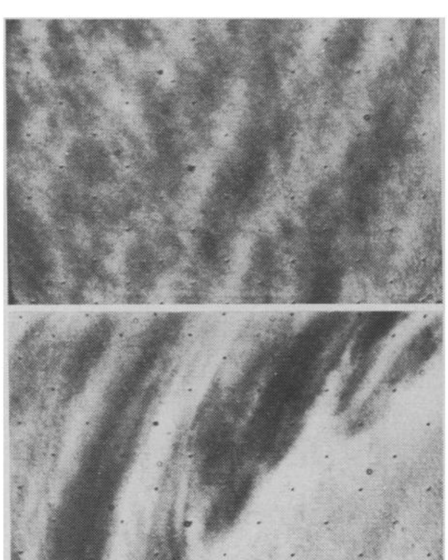

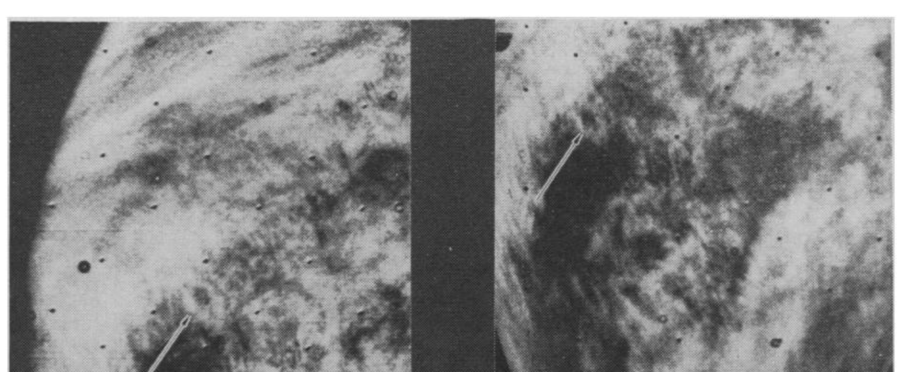

Fig. 7 (left). Venus has a mottled appearance in some areas of the equatorial region (top), while streaks and whorls are seen at high latitudes (bottom). Scale bar, 1000 km. Fig. 8 (above). High-resolution views taken 2 hours apart in the vicinity of the subsolar region of Venus, showing the persistence of the large cell (280 km) indicated by the arrows, and transitory nature of the smaller cells (170 km) to the right (east).

The temporal behavior of the markings suggests the formation and disappearance of condensate clouds rather than solely dust or photochemical products.

Nevertheless, we are unable to specify the probable constituents and their distribution within the clouds responsible for the observed markings. Hence, the inferences concerning atmospheric motion presented here must be regarded as tentative, subject to reinterpretation.

In order to provide a basic description of the observed motions, we introduce the nomenclature which is illustrated schematically in Fig. 9.

Subsolar disturbance. The obliquity of Venus is observed to be sufficiently small that no seasonal effects are anticipated (*14*). The subsolar portion of the equatorial region is characterized by the presence of cellular features, as shown in Fig. 8. In high-resolution mosaics, the larger (500 km), less distinct cells are bounded by dark edges. Some are polygonal in shape. Preliminary comparison of successive mosaics suggests lifetimes of a few hours at most. The interior of these cells is highly structured. A tenuous network of this type of cell has been traced over about 5 percent of the area of the planet near the subsolar point. Slightly smaller ($\sim$ 200 km) cells bounded by light material (as identified in Fig. 8) are also found which move with the wind and change markedly over a 2-

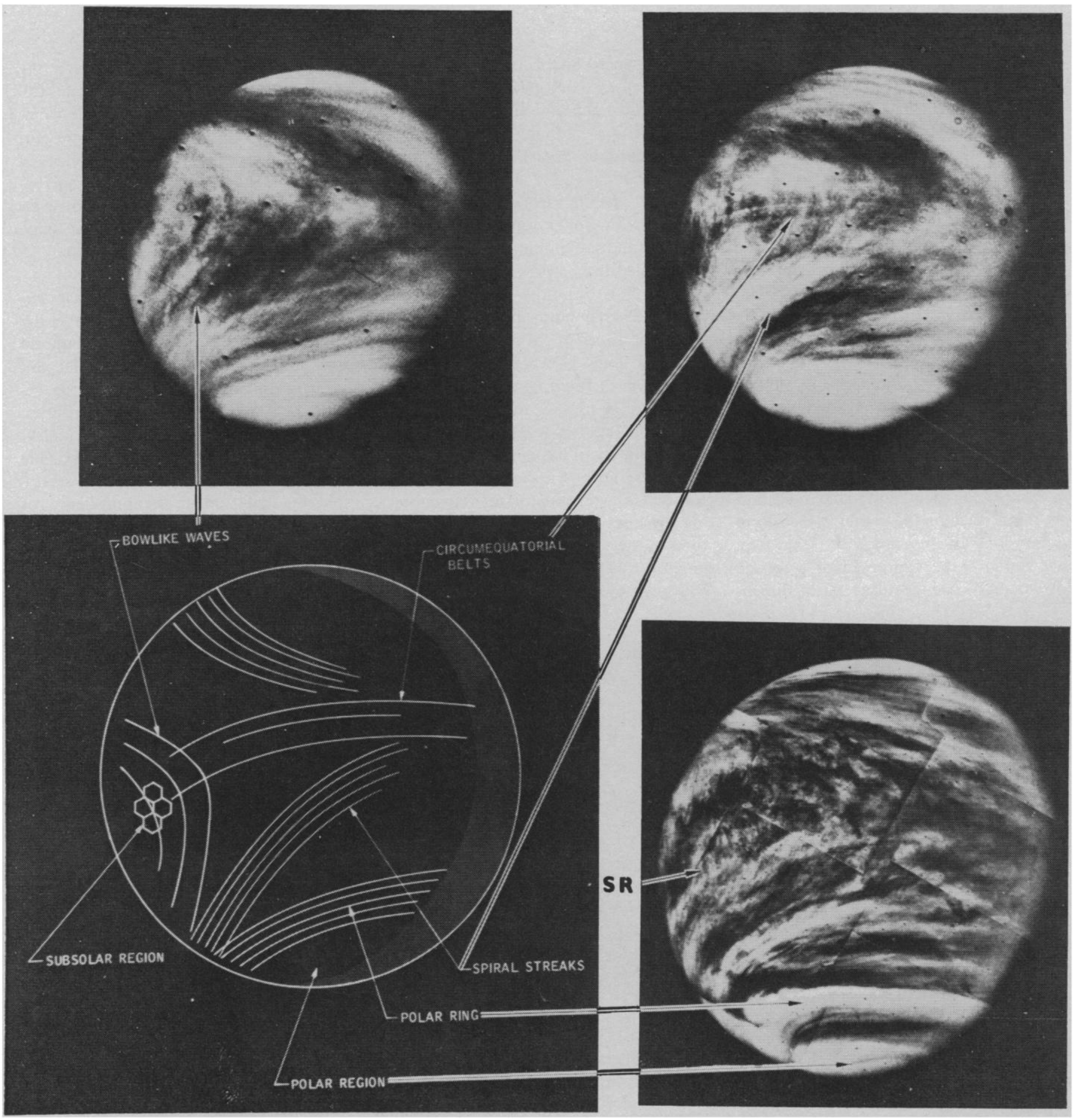

Fig. 9. The major features of the circulation pattern are identified in the sketch and are seen in most of the global pictures.

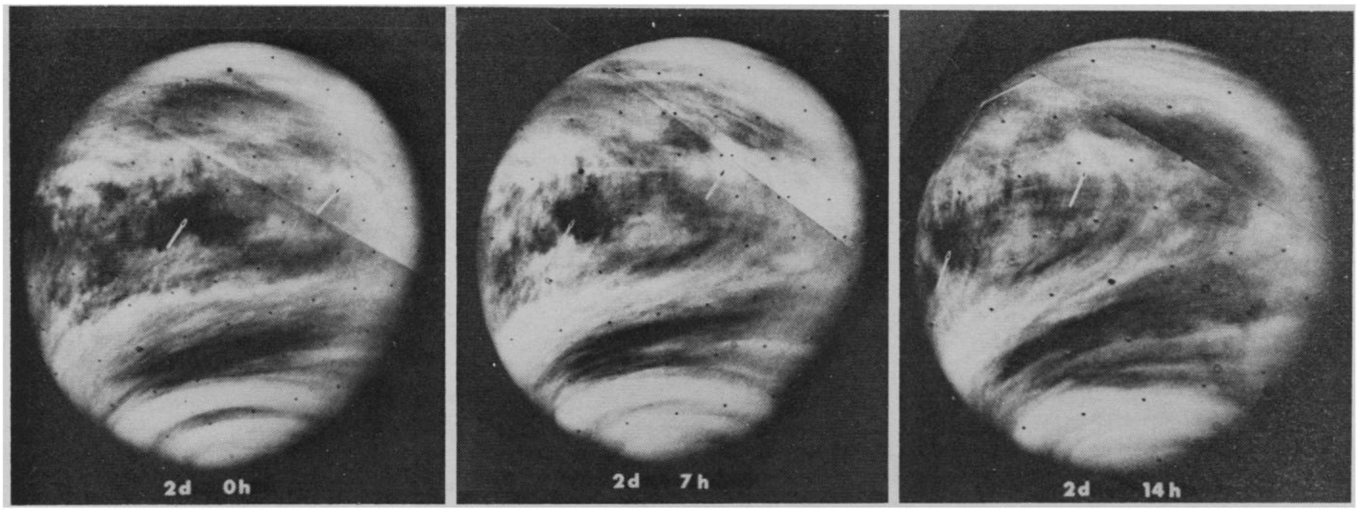

Fig. 10. Series of mosaics at 7-hour intervals showing the persistence of large light and dark markings (arrows) over a 14-hour period. The size of the features indicated is about 1000 km.

hour interval. The subsolar disturbance extends at its widest over ± 20° and at least 80° in longitude. The actual extent in longitude is not known, as the region extends beyond the limb. The subsolar point itself is located near the eastern extremity. The subsolar disturbance is locked to the sun-Venus line; it is continually being regenerated there, presumably in response to maximal solar heating.

Mid-latitude streamlined flow region. Conspicuous streaks originate in the equatorial region and spiral up to higher latitudes. In high-resolution mosaics, they are bordered on the equatorial side by finer streaks and, occasionally, whorls, suggestive of horizontal shear and turbulence. There are at least two major systems of jetlike spiral streaks in each hemisphere; one set appears to be symmetrical across the equator. The spiral features appear to be most prominent in mid-latitudes (~ ± 30°). They merge into a bright polar ring at 50° latitude after progressing some 200° to 300° of longitude around the planet. We have not observed any evidence of instability on a global scale in these features, nor evidence of structures similar to large-scale cyclonic eddies.

Figure 11 is a preliminary attempt to display the temporal appearance of the mid-latitude regions. The patterns are complex. Prominent dark, poleward markings sometimes appear fully formed when first viewed on the morning terminator. Other patterns seem to originate in the equatorial region.

Preliminary measurements of small-scale features as they move across the disk of the planet provide crude estimates of zonal motions. In the equatorial zone (outside of the subsolar disturbance) large discrete areas of light and dark material move primarily zonally at approximately 100 m/sec westward relative to the fixed planet, corresponding to an apparent equatorial retrograde rotation period of about 4 days. Smaller-scale features, however, do not always share this motion. Zonal components of about 80 to 90 m/sec in some cases are suggested. At higher latitudes motion is also primarily zonal.

The angular velocity of the markings increases with latitude although angular momentum diminishes somewhat with latitude. The suggestion of shear in the polar ring could mean an even higher zonal velocity. At 50° latitude the rotation period of the up-

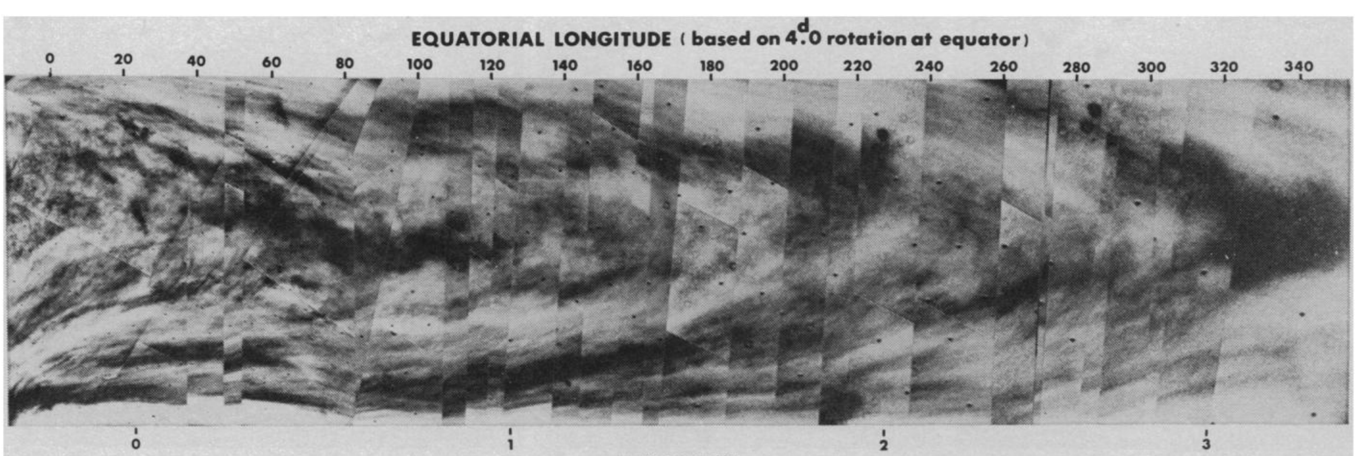

Fig. 11. Temporal display of the UV markings between + 40° latitude and − 50° latitude. The subsolar point moves from left to right in the picture as the planet rotates. The map contains considerable geometric distortion as the pictures were not rectified; however, it has been useful in studying the circulative pattern.

Fig. 12. Montage of global views on 1-day centers. Time progresses from top left to right, then down the page. The first frame (identical to the cover picture) is a mosaic of frames taken at encounter plus 1 day.

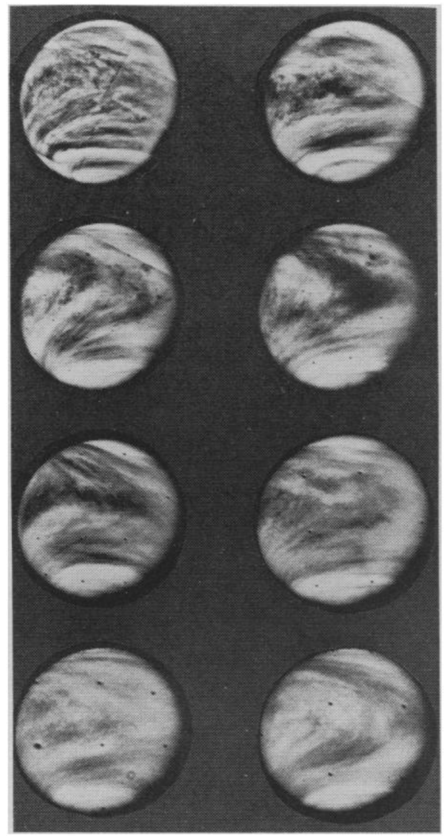

per atmosphere could be as short as 2 days.

We have not detected any measurable meridional motions in low-latitude regions. At higher latitudes (30° to 50°), particularly associated with the spiral streaks, poleward flow of the order of 10 m/sec is possibly indicated by the data, but must be substantiated by further analysis.

Polar region. The southern polar ring is perhaps the most distinctive and stable feature in the light markings. It encompasses a band of latitude 10° to 15° wide, with its equatorial side at 50° latitude. There are strong indications that a similar ring exists in the northern hemisphere, but the viewing geometry is unfavorable for a definite conclusion. Our preliminary impression is that the pole of atmospheric rotation is on the terminator (*14*). There is an indication of vortex structure in the streaks emanating from the poleward side of the edge of the polar region. Indeed, the entire polar region may be a vortex fed by meridional flow from the equatorial regions. A major systematic analysis of all the picture data is planned especially to elucidate the magnitude of possible meridional motions and the variation of angular momentum with latitude.

Interaction features. Very faint circumequatorial belts appear on some of the mosaics. Often three or four appear at one time between latitudes ± 20° and are parallel to latitude circles. The belts are less than 100 km in width, and appear to be moving rapidly around the globe in the same direction as the general motion and also drifting across latitude circles.

Dynamic interaction between the strong zonal flow and the solar-locked subsolar disturbance is evident. In some mosaics, we have noted the presence of darker features suggestive of bow waves generated by interaction with a "soft" obstacle (Fig. 9). These features move relative to the obstacle (unlike true bow waves). They are symmetrical about the equator, extending to at least ± 30° latitude and give the impression of being present in pairs. In one of the best examples they are separated by about 1000 km, each one being roughly 250 to 350 km in width. It is our impression that these features form at irregular intervals a few tens of degrees upwind of the subsolar disturbance and then propagate through (or over) that disturbance at roughly 80 percent of the average rotation speed.

Relation to ground-based UV photographs. The outstanding characteristic of the Mariner 10 pictures is a diverging pattern centered on the equator and opening in the direction of rotation, which is present throughout the entire 8-day period. Four days after encounter, a pronounced dark horizontal Y appeared on the equator, suggestive of the Y-shaped feature observed from the earth (Fig. 1). This feature was observed to rotate from morning terminator to limb at a rate consistent with an approximate 4-day rotation. The Y morphology recurred again 8 days after encounter.

Earth-based UV photographs often show a reversed C pattern in the eve-

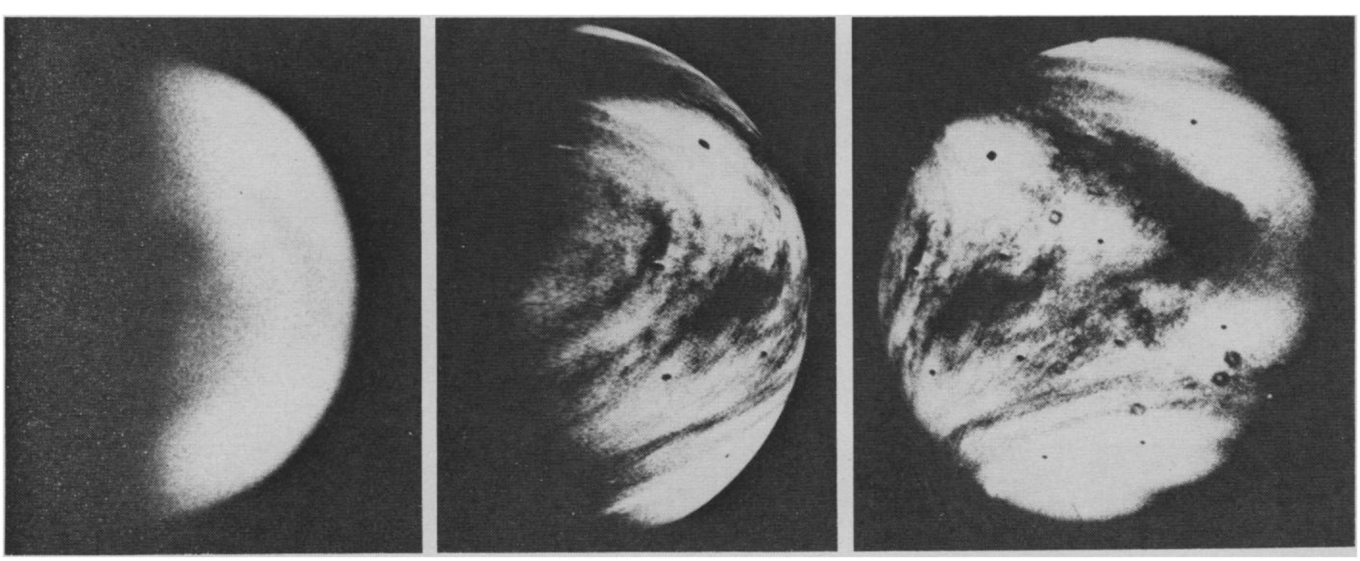

Fig. 13. (Left) Earth-based UV photograph of a reverse C feature on the evening terminator of Venus on 24 May 1967, 01:35 U.T. [Courtesy of New Mexico State University Observatory] (Center) Mariner 10 picture 4 days after encounter, projected on a globe and rephotographed to give an unforeshortened view of regions near the evening terminator. (Right) The same Mariner 10 picture viewed from the direction of the spacecraft.

ning terminator region (*6*). The same kind of morphology can be seen in a Mariner 10 picture after it was projected onto a globe and then rephotographed to give an unforeshortened view of regions near the evening terminator (Fig. 13). The reversed C is evidently associated with the Y feature and the bowlike wave structures to the west of the subsolar region. It is interesting to note that, in the numerous Earth-based UV photographs of Venus taken over the years, the Y and C features always open in the direction of rotation (*15*). Very long term stability is suggested for the diverging patterns so apparent in the 8 days of Mariner 10 observations. However, these preliminary results do not provide an "explanation" of the markings.

Characteristics of the limb, terminator, and cusp. Photographs of the cusps, terminator, and limb were acquired at very high spatial resolution (Fig. 14). The cusp appears devoid of small-scale structure, indicating a very homogeneously stratified medium. There is no evidence of shadowing or other horizontal brightness variation in the terminator region. At the low sun angles involved, this observation implies the absence of opaque shadow-casting clouds with vertical relief greater than about 20 m relative to any overlying clear atmosphere.

A sequence of 45 pictures of the limb of Venus in UV and orange filters was acquired from equator to polar latitudes at resolutions better than 1 km. Of these, ten have been investigated for analysis of any limb haze structure. Figure 15 shows four high-resolution views of the limb near the equator. In the orange frames, highly stratified layers ~ 1 km thick are found. There is a suggestion that the vertical structure is different at locations ~ 1000 km apart. Some UV frames also show evidence of layering.

Inferred vertical structure. The presence of cellular structures in the subsolar region suggests to us the presence of large-scale convection. In that region at least, we may be seeing down to the 100-mbar pressure level or deeper because the Mariner 10 radio occultation suggests a temperature inversion at ~ 100 mbar with a steep lapse rate below (*16*). The limb photographs apparently refer to a region much higher in the atmosphere. As a lower limit we take the UV and orange limbs to be defined by a slant optical path of unity

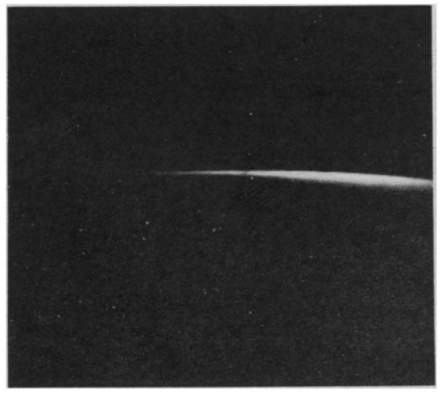

Fig. 14. View of the cusp region. The dark markings in the cusp are artifacts in the imaging system.

in rayleigh scattering. We find they correspond to regions in the atmosphere no lower than the 10-mbar and 90-mbar pressure levels, respectively. The existence of stratification in some UV limb pictures indicate that haze cloud particles are located up to the 10-mbar level and perhaps higher, consistent with the visual transit measurements (*9*).

Preliminary measurements of the curvature of the limb in selected frames indicate a haze layer radius of about 6130 km in both UV and orange light. Agreement between four different frames is within ± 2 km, but it is difficult at this time to estimate possible systematic errors. Comparing these data with the radio occultation results (*16*), we infer that both the UV and orange limbs are defined by a level in the stratosphere approximately 15 km above the tropopause and near the 10-mbar level. There is also a preliminary indication of similar haze structure in orange and UV frames taken near a latitude of 22° north (Fig. 15, c and d), again suggesting the presence of a particulate haze at or above the 10-mbar level in both colors.

Very thin, highly stratified limb hazes are indicative of the great stability in the atmosphere at these levels. Presumably the vertical eddy diffusivity is similar to, or less than, that found in the earth's stratosphere where similar phenomena occur. The resolution of the cusp pictures is rather low (~ 15 km). However, we can infer from these pictures that gross vertical separation into layers in the stratosphere more than 15 km thick does not occur.

The lack of shadowing in the terminator frames is consistent with the presence of an enveloping thin haze in the stratosphere. Any layers of cloud with well-defined vertical relief must be deep enough in the atmosphere so that at low sun angles the sunlight has been diffused enough by the overlying haze that shadows are effectively absent. At present, we see no basic conflict with recent models of the cloud structure (*17*) which require a stratospheric haze layer near the 20- to 50-mbar level with a vertical optical depth of ~ 2 above an optically dense second deck near the 200-mbar level.

Discussion of atmospheric circulation. Despite the preliminary nature of the data, the patterns and motions of the UV markings suggest a spectrum of models for planet-wide atmospheric circulation which are useful to discuss in order to develop a frame of reference for subsequent data analysis and future missions.

Some time ago, ground-based observations raised a fundamental question about atmospheric circulation on Venus: What is the source of angular momentum for rapidly moving UV clouds? A non-axisymmetric flow mechanism is needed. Schubert and Whitehead (*18*), followed by Gierasch (*19*) and Malkus (*20*), developed the "moving flame" model for Venus. Periodic solar heating of the top of the atmosphere results in cellular motion ultimately leading to uniform zonal flow. Non-axisymmetric motion takes place in vertical planes. Meridional motions are neglected.

To reconcile such two-dimensional concepts with the observed patterns of markings, it would be necessary to regard the spiral markings primarily as wavelike disturbances (not streamlines) which move with the mean zonal flow. The markings obviously are disrupted by the subsolar disturbance zone, but this is not taken to be any indication of divergence in flow. Figure 11, with its herringbone pattern, would be interpreted as somewhat like the result of rotating a cylinder with painted, or at least recurrent, markings (like a rotating barber's pole in which zonal motion gives the illusion of meridional motion).

The three-dimensional implication of the moving flame concept was considered very briefly by Malkus (*20*); he noted the possibility that a weak Hadley cell could develop near the top of the atmosphere and, by virtue of the equator-to-pole temperature contrast, transfer energy and angular momentum to higher latitudes. To apply this kind of interpretation, the spiral streaks of

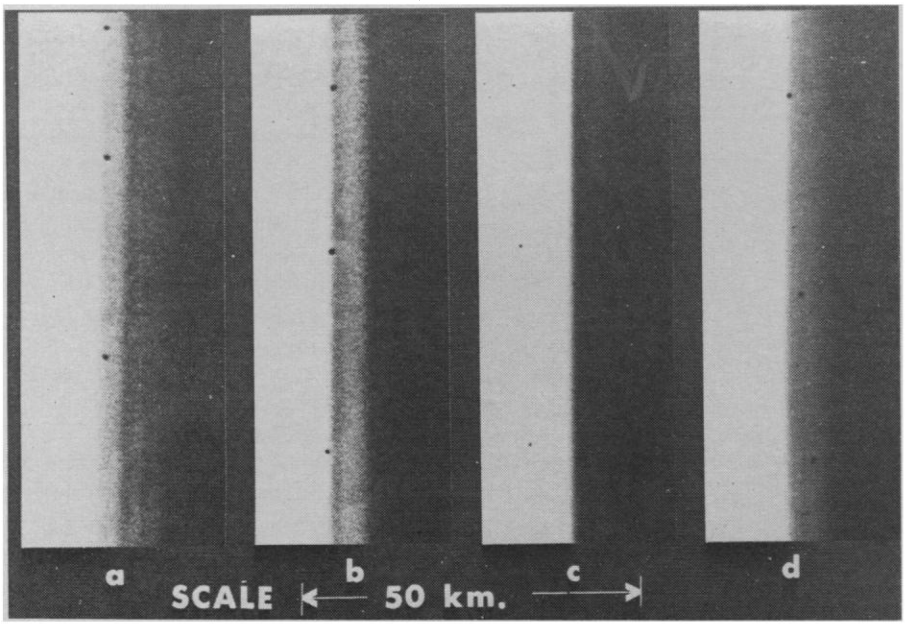

Fig. 15. Four views of the limb. Pictures (a) and (b) were taken through the orange filter near the equator; the two to the right are (c) orange and (d) UV photographs taken at 22°N latitude. All four pictures show structure indicating the presence of particulate matter in the stratosphere.

the mid-latitude streamline flow region would be inferred to be streamlines in this Hadley cell in a coordinate frame rotating with the mean equatorial motion. The spiral streaks presumably are clouds associated with disturbances induced in the Hadley flow by interaction between the equatorial flow and the subsolar disturbance. Both Malkus (*20*) and Geriasch *et al.* (*21*) allude to the possibility of gravity waves arising from the interaction of zonal flow and the subsolar region. The bowlike waves observed in the subsolar disturbance indeed are suggestive of some such interaction.

Carrying the impression of meridional motion further, the spiral streaks and general divergent pattern can be taken as evidence of an unexpectedly large influence of the subsolar region on global circulation. Great significance would be attached to the kinetic energy generated by velocity divergence in the subsolar high-pressure area; convection cells are interpreted as indicating a higher temperature and therefore a higher pressure. The resultant local meridional pressure gradients would imply velocity divergence and strong cross-isobaric flow to accelerate the zonal wind toward the poles; the spiral streaks are interpreted as associated jet streams. The kinetic energy sink is in the polar vortices due to velocity convergence at low pressure. As a further speculation, the bright polar ring would represent excess condensation associated with a kinetic energy maximum there. The bowlike waves are taken to be clear evidence of the imbalance between the pressure excess in the subsolar area and the mean zonal flow. Angular momentum conservation requires that poleward flow be deflected right in one hemisphere and left in the other. Thus, both flows would combine to add momentum in the same zonal direction. Equatorward return flow and also weak zonal counterflow at deeper levels are required to maintain the planetary angular momentum balance.

Thus, one extreme interpretation minimizes the importance of suggestions in the pictures of departures from uniform zonal flow. They are assigned at most to a superficial Hadley cell at the top of the atmosphere. The other extreme interpretation maximizes the implications of possible divergence of zonal flow and convergence at the pole, which could result from a persistent sun-locked high-pressure anomaly. Deep stirring of the atmosphere return flow is implied. At one extreme, the subsolar disturbance mainly generates cloud patterns; non-axisymmetric motion takes place only in vertical planes. At the other, the subsolar disturbance is a primary element of the global circulation system and non-axisymmetric flow is partly meridional as well.

To proceed further in interpretation, we will have to fully exploit the Mariner 10 television data, especially regarding evidence of meridional motions and variation of angular momentum with latitude.

Implications for future studies. Such disparate interpretations imply significantly different vertical temperature and wind profiles in equatorial and polar regions. Direct measurements of these and other atmospheric parameters from carefully targeted entry probes can provide a clear-cut choice—or point toward presently unimagined possibilities. In addition, in situ measurement of the cloud particle composition high in the atmosphere will probably be required for a clear understanding of the detailed origin of the UV markings. Certainly, additional UV imaging of Venus from an orbiter can now be regarded as a powerful tool for atmospheric research. Hence, even very preliminary assessment of the television pictures from Mariner 10 carries implications for the Venus Pioneer program of the United States scheduled for 1977 and 1978. In addition, the Soviet Union may plan future Venera systems with much larger spacecraft, comparable to those used at Mars in 1971–1972 and 1974. An exciting era of exploration of our nearest planetary neighbor is emerging in which imaging can play a significant scientific role.

BRUCE C. MURRAY
California Institute of Technology, Pasadena 91109

MICHAEL J. S. BELTON
Kitt Peak National Observatory, Tucson, Arizona 85717

G. EDWARD DANIELSON
Jet Propulsion Laboratory, Pasadena, California 91109

MERTON E. DAVIES
Rand Corporation, Santa Monica, California 90401

DONALD GAULT
Ames Research Center, Moffett Field, California 94035

BRUCE HAPKE
University of Pittsburgh, Pittsburgh, Pennsylvania 15260

BRIAN O'LEARY
Hampshire College, Amherst, Massachusetts 01002

ROBERT G. STROM
University of Arizona, Tucson 85726

VERNER SUOMI
University of Wisconsin, Madison 53706

NEWELL TRASK
U.S. Geological Survey, Reston, Virginia 22092

References and Notes

1. The gravitational field of Venus was used to reduce the heliocentric velocity of the spacecraft, following a suggestion made in 1963 by M. A. Minovitch, who was then a graduate student at the University of California, Los Angeles.
2. B. C. Murray *et al.*, *Icarus* **15**, 153 (1971).
3. F. E. Ross, *Astrophys. J.* **68**, 57 (1928).
4. C. Boyer and H. Camichel, *Ann. Astrophys.* **24**, 53 (1961).
5. C. Boyer and P. Guerin, *Icarus* **11**, 338 (1969).
6. A. H. Scott and E. J. Reese, *ibid.* **17**, 589 (1972).
7. B. Guinot and M. Feisael, *J. Observ.* **51**, 13 (1968); W. Traub and N. Carleton, paper presented at the NATO Advanced Study Institute, Istanbul, Turkey (1972). These authors have informed us that the spectroscopic data may indicate a more complicated situation than a simple equatorial mass motion of approximately 100 m/sec (private communication).
8. M. Y. Marov, V. S. Avduevsky, V. V. Kerzhanovich, M. K. Rozhdestvensky, N. F. Borodin, O. L. Ryabov, *J. Atmos. Sci.* **30**, 1210 (1973).
9. R. M. Goody, *Planet. Space Sci.* **15**, 1817 (1967).
10. This corresponds to four optical depths, an extreme estimate of maximum depth of visibility.
11. H. Masursky *et al.*, *Icarus* **12**, 10 (1970).
12. The original plans called for picture-taking for 16 days, but with an extended gap at 3 days. As it turned out, we achieved 8 days of almost uniform coverage instead.
13. D. L. Coffeen, in *Planetary Atmosphere*, C. Sagan, T. C. Owen, H. J. Smith, Eds. (Reidel, Dordrecht, Netherlands, 1971), p. 84.
14. The atmospheric rotation pole appears to be oriented parallel to the planetary rotational pole. However, detailed processing and measurements will be necessary to determine the relationship precisely. Any differences would be highly significant for a dynamical understanding of the atmosphere.
15. B. A. Smith, private communication.
16. H. T. Howard *et al.*, *Science* **183**, 1297 (1974).
17. W. A. Traub and N. Carleton, *Bull. Am. Astron. Soc.* **3**, 278 (1971); J. E. Hansen and A. Arking, *Science* **171**, 669 (1971).
18. G. Schubert and J. A. Whitehead, *Science* **163**, 7172 (1969).
19. P. Gierasch, *Icarus* **13**, 25 (1970).
20. W. V. R. Malkus, *J. Atmos. Sci.* **27**, 529 (1970).
21. P. J. Gierasch, A. P. Ingersoll, R. T. Williams, *Icarus* **19**, 473 (1973).
22. We acknowledge the ingenuity, diligence, and dedication of the many engineers and scientists of the Jet Propulsion Laboratory who have contributed to the Mariner 10 television experiment. In particular the skilled staff of the Space Photography Section, the Image Processing Laboratory, the Mission Test Computer, and the Mission Test Information System have played a major role in our work. James Anderson and Michael Malin of the California Institute of Technology, Robert Krauss of the University of Wisconsin, and Ken Klaasen and Robert Toombs of the Jet Propulsion Laboratory made major contributions. It has been a special privilege to work with Gene Giberson, manager of the Mariner-Venus-Mercury Project, and his able staff. Andrew Ingersoll of the California Institute of Technology supplied valuable criticism. Contribution No. 2458 of the Division of Geological and Planetary Sciences, California Institute of Technology, Pasadena 91109. Research sponsored in part by NASA contract NAS 7-100. Kitt Peak National Observatory is operated by AURA, Inc., under contract to the National Science Foundation.

4 March 1974

Ultraviolet Observations of Venus from Mariner 10: Preliminary Results

Abstract. *An objective grating spectrometer on Mariner 10 has measured airglow in the wavelength range 200 to 1700 angstroms. The data reveal the presence of significant concentrations of hydrogen, helium, carbon, and oxygen atoms in the upper atmosphere of Venus. A preliminary analysis of the hydrogen data indicates an exospheric temperature of 400°K. There is evidence for intense airglow emission at wavelengths longward of 1350 angstroms; the nature of this emission is unclear, but the radiation is spatially extensive and detectable on both day and night sides of the planet.*

The Mariner 10 payload included an objective grating spectrometer designed to measure airglow radiations from Venus and Mercury in the spectral range 200 to 1700 Å. A set of channel electron multipliers was used to detect radiation at ten selected wavelengths, with a spectral resolution of 20 Å. In addition, the spectrometer incorporated a pair of zero-order channels with effective band passes of 200 to 1500 and 1150 to 1700 Å, respectively. A summary of the various wavelengths, including information on possible radiating species, is given in Table 1. A more detailed description of the experiment will be presented elsewhere (*1*).

The spectrometer was mounted on the spacecraft scan platform, behind a sun shade. Observations were carried out in two modes, illustrated schematically in Fig. 1. In the first mode, the scan platform was placed in a fixed position and the spacecraft motion and limit cycle provided the desired change in the instrumental field of view (Fig. 1a). In the second mode, the clock coordinate (*2*) was fixed at a value corresponding to the center of the planetary disk, while the scan platform was moved in cone such that the field of view passed through successive levels of the atmosphere (Fig. 1b). The instrument has a field of view which measures 3° by ⅛°, with the larger dimension associated with the clock direction.

Observations were carried out in the fixed platform mode during the period 6 hours to 30 minutes before Venus encounter. The orientation of the slit, projected on the planet, is shown in Fig. 1a. The data obtained from the 1216 Å, 584 Å, and zero-order channels are given in Fig. 2. There is a perceptible rise in the Lyman alpha (1216 Å) channel prior to dark limb passage, indicating the presence of an extensive atmosphere of atomic hydrogen around Venus. There is evidence also for helium emission on the dark side of the planet, as may be inferred from the 584-Å record in Fig. 2. One would expect that the counting rate associated with sky background at 584 Å should vanish after dark limb passage. However, the counting rate in the 584-Å channel remained finite, and climbed rapidly as the field of view approached the bright limb. Extensive emission is evident also in the longer wavelength zero-order channel, Z02. The intensity of this radiation exceeds the sum of the intensities measured in all of the high-resolution channels. The nature of the emission and its mode of excitation remain unclear but should be clarified by a more extensive analysis of the data.

Observations of the bright limb were carried out from 9 minutes to 14 minutes after encounter, using the fixed platform observing mode. Strong emissions were detected at 584, 1048, 1216, 1304, 1480, and 1657 Å, and the variation of these emissions was measured as a function of altitude, as the field of view passed through successively higher atmospheric layers. Analysis of these data should eventually provide information on atmospheric temperature and will allow a careful study of the physical and chemical processes that regulate conditions in Venus's upper atmosphere. We are unable, however, to report on these matters at this time: Necessary pointing information and trajectory data were unavailable when this report was prepared.

A series of observations of the hydrogen corona were performed using the scanning mode at approximately 3 and 6 hours after encounter. The initial sequence consisted of four spatial scans, across the disk and off the limb to an altitude of 25,000 km. The scan sequence is shown schematically in Fig. 1b. The field of view of the spectrometer, projected on the planet, had a spatial extent of 230 km in the direction of the scan. The data from the four scans at 3 hours, superimposed to improve the statistics, are shown in Fig. 3. Figure 3 also includes, for comparison, Lyman alpha observations of